Anal. Chem. **2006,** *78,* 5158−5164

Electroporation of Mammalian Cells in a Microfluidic Channel with Geometric Variation

Hsiang-Yu Wang and Chang Lu*

Department of Agricultural and Biological Engineering, School of Chemical Engineering, Purdue University, West Lafayette, Indiana 47907

Electroporation has been widely used to load impermeant exogenous molecules into cells. Rapid electrical lysis based on electroporation has also been applied to analyze intracellular materials at single-cell level. There has been increasing demand to implement electroporation in a microfluidic format as a basic tool for applications ranging from screening of drugs and genes to studies of intracellular dynamics. In this report, we have developed a simple technique to electroporate mammalian cells with high throughput on a microfluidic platform. In our design, electroporation only happened in a defined section of a microfluidic channel due to the local field amplification by geometric variation. The time of exposure of the cells to this high field was determined by the velocity of the cells and the length of the section. The change in the cell morphology during electroporation was observed in real time. We determined that electroporation of Chinese hamster ovary cells occurred when the local field strength was increased to ~400 V/cm. The internalization of membrane-impermeant molecules (SYTOX green) with cell viability preserved was also carried out to demonstrate transient electropermeabilization. The influence of the operational parameters of the device on cell viability was determined. A large percentage of cells remained viable after electroporation when the parameters were tuned. We also studied rapid cell lysis when the field intensity was in the range of 600−1200 V/cm. The rupture of cell membrane happened within 30 ms when the field strength was 1200 V/cm. Given the simplicity, high throughput, and high compatibility with other devices, this microfluidic electroporation technique may increase the application of microfluidic systems in screening of drugs and biomolecules and chemical cytometry.

The effect of electrical field on the membranes of living cells has been under investigation since the 1960s and 1970s.[1−5] It was found that an applied electrical field could reversibly as well as irreversibly break down cell membranes in vitro. An external electrical field modulates the cell membrane potential difference. Transmembrane potential, ΔV_m, induced in a cell by an applied field, E, can be described using the equation[6,7]

$$\Delta V_m = \delta E r \cos\phi \quad (1)$$

In the equation, δ is the weighting factor that quantifies the impact of the cell on the extracellular field distribution while r and ϕ represent the cell radius and polar angle with respect to external field, respectively. When the transmembrane potential ΔV_m reaches ~250 mV, the membrane gets permeable due to formation of pores.[8]

Electroporation has been traditionally used to facilitate delivery of impermeant molecules into cells. By transiently and reversibly permeabilizing cells, genes and drugs have been delivered into cells in vitro and in vivo based on electroporation. [6,9−15] More recently, a number of groups have explored using electrical field to irreversibly disrupt the cell membrane (cell lysis).[16−23] Electrical cell lysis has gained substantial popularity in the community due

* Corresponding author. Tel: 765-494-1188. Fax: 765-496-1115. E-mail: changlu@purdue.edu.

(1) Coster, H. *Biophys. J.* **1965**, *5*, 669−686.
(2) Crowley, J. *Biophys. J.* **1973**, *13*, 711−724.
(3) Sale, A.; Hamilton, W. *Biochim. Biophys. Acta* **1967**, *148*, 781−788.
(4) Sale, A.; Hamilton, W. *Biochim. Biophys. Acta* **1968**, *163*, 37−43.
(5) Zimmermann, U.; Pilwat, G.; Riemann, F. *Biophys. J.* **1974**, *14*, 881−899.
(6) Neumann, E.; Schaefer-Ridder, M.; Wand, Y.; Hofschneider, P. *EMBO J.* **1982**, *1*, 841−845.
(7) Neumann, E.; Kakorin, S.; Tsoneva, I.; Nikolova, B.; Tomov, T. *Biophys. J.* **1996**, *71*, 868−877.
(8) Teissie, J.; Rols, M. P. *Biophys. J.* **1993**, *65*, 409−413.
(9) Potter, H.; Weir, L.; Leder, P. *Proc. Natl. Acad. Sci. U. S. A.* **1984**, *81*, 7161−7165.
(10) Fromm, M.; Taylor, L.; Walbot, V. *Proc. Natl. Acad. Sci. U. S. A.* **1985**, *82*, 5824−5828.
(11) Toneguzzo, F.; Keating, A. *Proc. Natl. Acad. Sci. U. S. A.* **1986**, *83*, 3496−3499.
(12) Prausnitz, M.; Bose, V.; Langer, R.; Weaver, J. *Proc. Natl. Acad. Sci. U.S. A.* **1993**, *90*, 10504−10508.
(13) Mir, L.; Orlowski, S.; Belehradek, J.; Paoletti, C. *Eur. J. Cancer* **1991**, *27*, 68−72.
(14) Belehradek, M.; Domenge, C.; Luboinski, B.; Orlowski, S.; Belehradek, J.; Mir, L. *Cancer* **1993**, *72*, 3694−3700.
(15) Ramirez, L.; Orlowski, S.; An, D.; Bindoula, G.; Dzodic, R.; Ardouin, P.; Bognel, C.; Belehradek, J.; Munck, J.; Mir, L. *Br. J. Cancer* **1998**, *77*, 2104−2111.
(16) Han, F. T.; Wang, Y.; Sims, C. E.; Bachman, M.; Chang, R. S.; Li, G. P.; Allbritton, N. L. *Anal. Chem.* **2003**, *75*, 3688−3696.
(17) Cheng, J.; Sheldon, E. L.; Wu, L.; Uribe, A.; Gerrue, L. O.; Carrino, J.; Heller, M. J.; O'Connell, J. P. *Nat. Biotechnol.* **1998**, *16*, 541−546.
(18) Lee, S. W.; Tai, Y. C. *Sens. Actuators, A* **1999**, *73*, 74−79.
(19) McClain, M. A.; Culbertson, C. T.; Jacobson, S. C.; Allbritton, N. L.; Sims, C. E.; Ramsey, J. M. *Anal. Chem.* **2003**, *75*, 5646−5655.
(20) Gao, J.; Yin, X. F.; Fang, Z. L. *Lab Chip* **2004**, *4*, 47−52.
(21) Lu, H.; Schmidt, M. A.; Jensen, K. F. *Lab Chip* **2005**, *5*, 23−29.
(22) Munce, N. R.; Li, J.; Herman, P. R.; Lilge, L. *Anal. Chem.* **2004**, *76*, 4983−4989.
(23) Khine, M.; Lau, A.; Ionescu-Zanetti, C.; Seo, J.; Lee, L. P. *Lab Chip* **2005**, *5*, 38−43.

10.1021/ac060733n CCC: $33.50
Published on Web 06/20/2006

to its speed and reagentless procedure compared to chemical and mechanical methods.[24−26] Electrical lysis provides a basis for biological assays based on intracellular contents. Chemical analysis of intracellular contents such as nucleic acids and proteins is of significant interest to the biological, medical, and pharmaceutical communities. Detection of abnormal genes and proteins in the intracellular materials provides important clues for early disease diagnosis.[27,28] Monitoring of cell cycle-dependent proteins is critical in the studies of oncology, stem cell research, and developmental biology.[29,30]

A number of innovative strategies have been developed to electroporate cells on a microfluidic platform.[17−23,31−33] In most reports, pulsed or ac voltage was applied to generate the field necessary for electroporation.[17,18,21,31−33] High-density microscale electrode arrays have been used to decrease the gap between electrodes and to minimize the overall voltage needed.[18,21] In another scheme, microfluidic structures with subcellular dimensions were applied to focus the electrical field on a deformed membrane area to produce electroporation with a low field.[22,23] When cell lysis is carried out in a direct current (dc) field, the major challenge is the generation of bubbles due to water electrolysis and Joule heating associated with the high field strength needed.[19,20] In a previous work, a combination of 400 V/cm ac field and 500 V/cm dc field was applied to provide a sufficient field strength for lysis without bubbling.[19]

Recent progress in microfluidics reveals the possibility of creating highly integrated systems that are capable of high-throughput screening a large number of chemical and biological samples in a parallel fashion.[34,35] Electroporation will be an indispensable tool for delivery of drugs and genes into cells for screening purpose on a microfluidic platform. Furthermore, combining with separation methods such as microchip electrophoresis, rapid lysis based on microfluidic electroporation will enable analysis of cellular analytes, such as nucleic acids and proteins, with high sensitivity and high temporal resolution at the single-cell level. All these needs will likely make microfluidic electroporation a very basic tool for a wide range of applications.

In this study, we present a high-throughput microfluidic electroporation device. The device was capable of producing either transient permeabilization of a cell membrane or irreversible cell lysis, dependent on the voltage applied. We applied a continuous dc voltage instead of electrical pulses to produce the electroporation field in a microfluidic channel. There were alternating high and low field intensities in different sections due to the geometry of the channel.[36,37] Electroporation occurred exclusively in a geometrically defined section of the channel. The duration for cells to expose to the electroporation field was varied by adjusting their velocity in the microscale flow. We used Chinese hamster ovary (CHO) cells as the model in our study. Electroporation occurred when the local field strength was increased to ∼400 V/cm. We studied electroporation of CHO cells under varying field intensities and durations. Both transient electropermeabilization and rapid electrical lysis were demonstrated in this work.

EXPERIMENTAL SECTION

Microchip Fabrication. Microfluidic devices were fabricated based on PDMS using a standard soft lithography method.[38] The microscale patterns were first created using a computer-aided design software (FreeHand MX, Macromedia, San Francisco, CA) and then printed out on high-resolution (5080 dpi) transparencies. The transparencies were used as photomasks in photolithography on a negative photoresist (SU-8 2010, MicroChem Corp., Newton, MA). The thickness of the photoresist and hence the depth of the channels was ∼33 μm (measured by a Sloan Dektak3 ST profilometer). The pattern of channels in the photomask was replicated in SU-8 after exposure and development. The microfluidic channels were molded by casting a layer (∼5 mm) of PDMS prepolymer mixture (General Electric Silicones RTV 615, MG Chemicals, Toronto, ON, Canada) with a mass ratio of A:B = 10:1 on the photoresist/silicon wafer master treated with tridecafluoro-1,1,2,2-tetrahydrooctyl-1-trichlorosilane (United Chemical Technologies, Bristol, PA). The prepolymer mixture was cured at 85 °C for 2 h in an oven and then peeled off from the master. Glass slides were cleaned in a basic solution (H_2O:NH_4OH (27%):H_2O_2 (30%) = 5:1:1, volumetric ratio) at 75 °C for 1 h and then rinsed with DI water and blown dry. The PDMS chip and a glass slide were rendered hydrophilic by oxidizing them using a Tesla coil (Kimble/Kontes, Vineland, NJ) in atmosphere. The PDMS chip was then immediately brought into contact against the slide after oxidation to form closed channels.

Reagents and Cell Culture. Chinese hamster ovary (CHO-K1) cells have been employed in all our experiments. Cells were incubated at 37 °C, under 5% CO_2 in Dulbecco's modified Eagle's medium (Mediatech Inc.) supplemented with 10% (v/v) fetal bovine serum (Sigma, St. Louis, MO), penicillin (100 units/mL, Sigma), and streptomycin (100 μg/mL, Sigma). To maintain cells in the exponential growth phase (∼1 × 10^6 cells/mL), they were diluted at a ratio of 1:5−1:8 every 2 days. The harvested cells were centrifuged at 300*g* for 10 min to remove the supernatant. Electroporation buffer (10 mM phosphate buffer and 250 mM sucrose, pH 7.4) was used to suspend the cell pallet for the subsequent experiments. To prevent clogging, the electroporation buffer was filtered with a 0.2-μm filter.

We demonstrated the introduction of membrane-impermeant exogenous molecules into cells during electroporation. SYTOX

(24) Belgrader, P.; Hansford, D.; Kovacs, G. T. A.; Vankateswaran, K.; Mariella, R.; Milanovich, F.; Nasarabadi, S.; Okuzumi, M.; Pourahmadi, F.; Northrup, M. A. *Anal. Chem.* **1999**, *71*, 4232−4236.
(25) Li, P. C. H.; Harrison, D. J. *Anal. Chem.* **1997**, *69*, 1564−1568.
(26) Taylor, M. T.; Belgrader, P.; Furman, B. J.; Pourahmadi, F.; Kovacs, G. T. A.; Northrup, M. A. *Anal. Chem.* **2001**, *73*, 492−496.
(27) Golub, T. R.; Slonim, D. K.; Tamayo, P.; Huard, C.; Gaasenbeek, M.; Mesirov, J. P.; Coller, H.; Loh, M. L.; Downing, J. R.; Caligiuri, M. A.; Bloomfield, C. D.; Lander, E. S. *Science* **1999**, *286*, 531−537.
(28) Yang, W. C.; Yeung, E. S.; Schmerr, M. J. *Electrophoresis* **2005**, *26*, 1751−1759.
(29) Krylov, S. N.; Zhang, Z. R.; Chan, N. W. C.; Arriaga, E.; Palcic, M. M.; Dovichi, N. J. *Cytometry* **1999**, *37*, 14−20.
(30) Hu, S.; Zhang, L.; Krylov, S.; Dovichi, N. J. *Anal. Chem.* **2003**, *75*, 3495−3501.
(31) Huang, Y.; Rubinsky, B. *Sens. Actuators, A* **2001**, *89*, 242−249.
(32) Huang, Y.; Rubinsky, B. *Sens. Actuators, A* **2003**, *104*, 205−212.
(33) Shin, Y. S.; Cho, K.; Kim, J. K.; Lim, S. H.; Park, C. H.; Lee, K. B.; Park, Y.; Chung, C.; Han, D. C.; Chang, J. K. *Anal. Chem.* **2004**, *76*, 7045−7052.
(34) Hansen, C. L.; Sommer, M. O. A.; Quake, S. R. *Proc. Natl. Acad. Sci. U. S. A.* **2004**, *101*, 14431−14436.
(35) Thorsen, T.; Maerkl, S. J.; Quake, S. R. *Science* **2002**, *298*, 580−584.
(36) Jacobson, S. C.; Culbertson, C. T.; Daler, J. E.; Ramsey, J. M. *Anal. Chem.* **1998**, *70*, 3476−3480.
(37) Plenert, M. L.; Shear, J. B. *Proc. Natl. Acad. Sci. U. S. A.* **2003**, *100*, 3853−3857.
(38) Duffy, D. C.; McDonald, J. C.; Schueller, O. J. A.; Whitesides, G. M. *Anal. Chem.* **1998**, *70*, 4974−4984.

green nucleic acid stain (MW ~600, 504/523 nm, Molecular Probes, Eugene, OR) is an excellent green fluorescent nuclear and chromosome counterstain that is impermeant to live cells and yields >500-fold fluorescence intensity enhancement upon nucleic acid binding. In this experiment, cells were harvested and then centrifuged to remove the medium. They were resuspended in the electroporation buffer with a concentration of 1×10^6 cells/mL. Two separate sets of tests were done. In one set of tests, SYTOX green was added to the cell sample in the electroporation buffer to create a concentration of 1 μM before the sample was delivered into the device for electroporation. In the other set of tests, the cell sample was delivered into the device and electroporated first. Then SYTOX green was added to the cell sample 1 h after the electroporation to achieve the same final concentration (1 μM). In all the tests, the cells were collected from the receiving reservoir and transferred to a 96-well plate immediately after electroporation. The fluorescent and nonfluorescent cells within a population of 500−1000 cells were enumerated 1.5 h after the electroporation under a microscope.

We also determined cell viability after electroporation using trypan blue exclusion. Cells were collected from the receiving reservoir (outlet) 1 h after the experiment. The cells were stained in the electroporation buffer containing 0.4 mM trypan blue for 10−15 min. Viable cells excluded trypan blue, while dead cells stained blue due to trypan blue uptake. After electroporation under a set of operational parameters, the percentage of viable cells was typically determined by observing 500−1000 cells under a microscope. It needs to be noted that we measured only short-term cell death (after 1 h) in this work. The long-term cell death (after 24 h or longer) may be different.[39]

For observing the leak of intracellular materials during electroporation, cells were loaded with a fluorogenic dye, calcein AM (MW ~995, 495/517 nm, Molecular Probes, Eugene, OR) at a concentration of 1 μg/mL in the electroporation buffer for 15 min. In live cells, the nonfluorescent calcein AM is converted to green fluorescent calcein, after acetoxymethyl ester hydrolysis by intracellular esterases. The fluorescent images of cells also enabled us to obtain the velocity of cells under different field strengths and infusion rates. The velocity was typically obtained based on image series containing at least 10 cells.

Phase Contrast and Fluorescence Microscopy. During the experiments, we observed the cells in the channel using a fluorescent microscope with phase contrast. The microfluidic device was mounted on an inverted fluorescence microscope (IX-71, Olympus, Melville, NY) with a 40× dry objective (NA = 0.40). The epifluorescence excitation was provided by a 100-W mercury lamp, together with bright-field illumination. The excitation and emission from cells loaded with calcein AM were filtered by a fluorescence filter cube (Exciter HQ480/40, emitter HQ535/50, and beam splitter Q505lp, Chroma Technology, Rockingham, VT). The images of the cells were taken with a CCD camera (ORCA-285, Hamamatsu, Bridgewater, NJ) at a frame rate of 16/33 Hz.

Microchip Operation. Prior to the experiments, the channels were flushed with the electroporation buffer for 15 min to condition the channels and remove impurities. When a slow velocity was desired for obtaining clear cell images, the flow of cells was induced by a liquid level difference between the two reservoirs. When accurate velocities of cells were needed, the inlet end of the channel was connected to a syringe pump (PHD infusion pump, Harvard Apparatus, Cambridge, MA) through plastic tubing, and the electrode (a Pt wire) on the inlet side was inserted into the reservoir through a hole poked by a needle with a diameter slightly smaller than that of the Pt wire (as shown in Figure 1b). The setup ensured the contact between the electrodes and the solution and in the meantime allowed the establishment of a pressure-driven flow. Flow rates ranging from 1.2 to 2.7 μL/min were provided during the experiments. The experiment typically lasted 5 min. A new device was used in each experiment to eliminate the effects of cell lysate adsorption on surface properties of the channel.

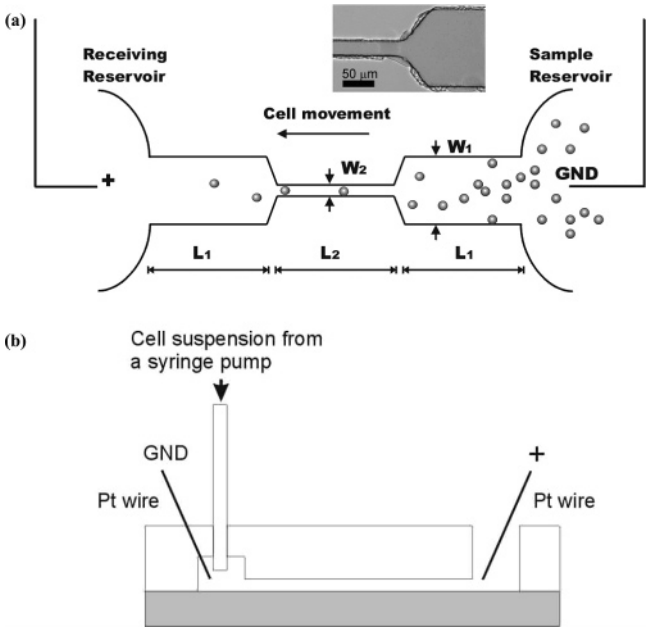

Figure 1. (a) Schematic of the electroporation device. Cells were loaded into the sample reservoir and flowed to the receiving reservoir in a dc field. Electroporation was confined in the narrow section of the channel due to the amplified field inside. The inset shows a microscope image of a part of a fabricated device. The devices used in this study have the following dimensions: $L_1 = 2.5$ mm, $L_2 = 2.0$ mm, $W_1 = 213$ μm, and $W_2 = 33$ μm. (b) The setup of the device when regulated flow rates were desired. The inlet of the channel was connected to a syringe pump through plastic tubing, and the electrode was inserted into the reservoir through the elastic PDMS wall.

RESULTS AND DISCUSSION

Design of the Device. The vast majority of the previous work on electroporation, in vitro or in vivo, has been demonstrated using pulsed electrical fields, especially when cell viability needed to be preserved. Exponentially decaying pulses or square wave pulses with width of 10 μs−20 ms have been typically applied to create transient permeation in the cell membrane. In this study, we developed a novel microfluidic device for electroporation based on continuous dc voltage. We applied geometric variation to a microfluidic channel to create a local high field in a geometrically defined section. We controlled the overall voltage across the channel so that only the field intensity in the defined section would produce electroporation. We were able to adjust the duration for the cells to be in the high field by controlling the velocity of the cells and the length of the electroporation section.

(39) Gabriel, B.; Teissie, J. *Biochim. Biophys. Acta* **1995**, *1266*, 171−178.

The schematic of the microfluidic electroporation device and setup are shown in Figure 1. The devices used in this study have the following dimensions: $L_1 = 2.5$ mm, $L_2 = 2.0$ mm, $W_1 = 213$ μm, and $W_2 = 33$ μm. Based on Ohm's law, when a dc voltage is applied at a conductor (in this case, a buffer-filled channel), the potential drop at individual sections of the conductor is proportional to its resistance within the section. Like any conductor, the resistance within a certain section of a microfluidic channel is determined by the conductivity, the length, and the cross sectional area. For a channel with an uniform depth and a varying width as shown in Figure 1a, the field strength E is different in different sections. The field strength in the wide section (E_1) and in the narrow section (E_2) can be calculated using the following equations.

$$E_1 = \frac{V}{2L_1 + L_2(W_1/W_2)} \tag{2}$$

$$E_2 = \frac{V}{2L_1(W_2/W_1) + L_2} \tag{3}$$

$$E_2/E_1 = W_1/W_2 \tag{4}$$

The width W_2 was always much smaller than W_1 in our design. This resulted in much higher field strength in the narrow section compared to those of the other two sections when a dc field was applied across the whole length of the device. Similar geometric variations have been shown to create local electrical field as high as 0.1 MV cm^{-1}.[36,37] The roughness at the edge of the channels was due to the quality of the photomask (high-resolution transparency). The roughness should not introduce major change in the width of the channel due to the small size of the intruding structures.

There were several unique advantages that made our device particularly suitable for high-throughput electroporation of cells. First, the instrumentation was extremely simple. A dc power supply replaced the pulse generator to apply the field and simple microfluidic channels generated alternating high and low fields by geometric variation. The arrangement of alternating low-field and high-field sections effectively decreased the overall voltage needed for the electroporation. Second, the associated microfabrication procedure was simple and low cost. Unlike previous reports, no microscale electrodes or structures with subcellular dimensions will be needed in our device.[18,21,31,32] Low-cost soft lithography was used for the fabrication. Third, in this design, the dimensions of the narrow section determined that cells were processed individually. It was possible to realize single-cell analysis to investigate the heterogeneity in the cell population. Finally, given the simplicity of the design, it will be very straightforward to integrate this device with other existent devices, forming high-density and large-scale parallel systems.

It needs to be noted that, when the cell density is very high in the electroporation buffer, the electric field in the narrow section may be disturbed by the presence of cells and become more complicated than what was suggested by eqs 2−4. Cells before permeabilization are essentially nonconducting, and their conductance increases dramatically upon electropermeabilization.[40] Such change will affect the local field strength in the narrow section. We did not observe any obvious change in the result with the number of cells in the narrow section in the study, possibly due to relatively low cell density and the fact that both the channel's width and depth were almost two times larger than the diameter of a single cell.

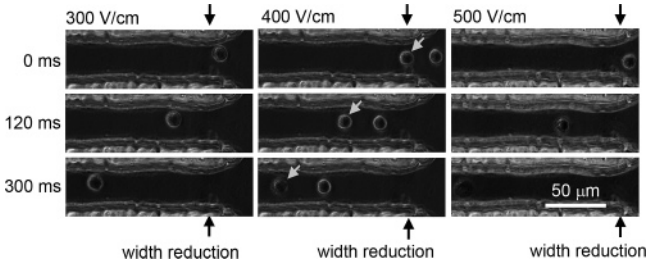

Figure 2. Image series showing the expansion in the cell diameter during electroporation. Low field strengths for E_2 (300−500 V/cm) were applied. The images were taken at a frame rate of 16 Hz. The arrows indicate where the width reduction occurs in the channel.

Expansion in the Cell Size due to Electroporation. One important indication of electroporation we observed was that the size of CHO cells increased when cells entered the narrow section of the channel with high field. It has been reported that the size of CHO cells increased by up to 30% after electroporation by electrical pulses (10 pulses of 5 ms and 800 V/cm at a frequency of 1 Hz).[41] Similar change in cell morphology has been reported in other work involving electroporation of other cell types.[33] Such increase was due to absorption of the buffer through the breached membrane. In our work, we did not observe significant change in the cell size when cells entered the wide sections from the sample reservoir. The field strength was zero in the reservoir and always lower than 200 V/cm in wide sections. However, the cell size visibly increased over time when cells entered the narrow section from the wide section when the field in the narrow section (E_2) was increased to ~400 V/cm. Since a continuous dc voltage was used, we were able to observe the increase in the cell size during electroporation in real time. In this experiment, the cells flowed through the channel under the influence of gravity with a velocity of 240−600 μm/s and the images were taken with a 60-ms interval in between. We were able to observe a channel length of ~250−400 μm in the camera's frame, next to the point where the width reduction occurred.

Figure 2 indicates that, at a time scale of 300 ms, we did not observe any change in the cell morphology when E_2 was 300 V/cm or below. Expansion in the cell size was clearly present when E_2 was increased to 400 V/cm. However, for this particular cell with E_2 at 400 V/cm, such expansion became pronounced mainly after the cell was in the field longer than 200 ms. Based on our observation of the increase in cell diameter, we determined that the threshold for CHO cell electroporation was ~400 V/cm. This result matches the electroporation threshold determined for CHO cells using electropulsation with a similar buffer system.[41] The fact that the cell size increased only at the entry of the narrow section confirmed our hypothesis that the field was locally amplified due to the geometry.

(40) Zimmermann, U.; Pilwat, G.; Riemann, F. *Biophys. J.* **1974**, *14*, 881−899.
(41) Golzio, M.; Mora, M.; Raynaud, C.; Delteil, C.; Teissie, J.; Rols, M. *Biophys. J.* **1998**, *74*, 3015−3022.

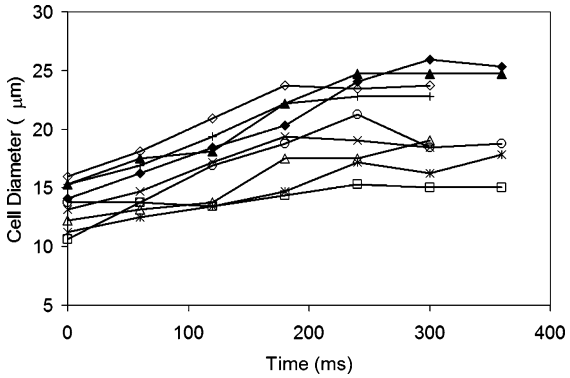

Figure 3. Change in the cell diameter over time during electroporation for 9 cells with different original sizes. E_2 was 500 V/cm.

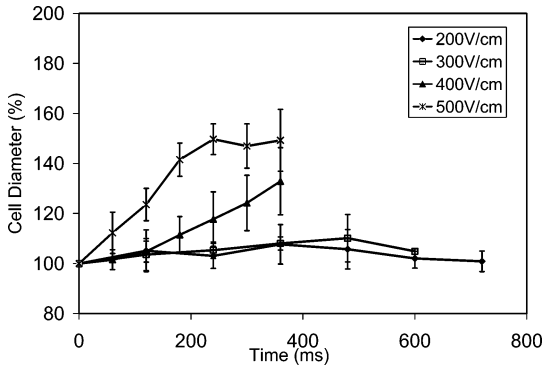

Figure 4. Percentile change in the cell diameter over time during electroporation with different field intensities for E_2. Each curve was generated by averaging data from 9 to 15 cells.

According to eq 1 and the literature, the larger the cell diameter, the lower the field strength threshold required for electroporation.[8] We studied whether the original cell diameter affected the expansion in the cell size during electroporation. In our experiments, we observed a number of cells (9−15) individually and recorded the change in the cell size over time for each cell when they entered the narrow section at different E_2. Figure 3 shows that, with E_2 at 500 V/cm and the original diameter of the cells (before they entered the narrow section) ranging from 10 to 16 μm, the rate of change in the cell size did not seem to correlate with the starting cell diameter. The data at other field intensities were similar. Presumably, although larger cells tend to be more susceptible to the field, it takes more influx to expand their diameters.

As shown in Figure 4, we averaged the percentile increase in the cell size over time based on data from 9 to 15 cells (of different sizes) taken at different field strengths E_2. The curves show that in general cells expanded more rapidly when E_2 was higher. There was only a moderate increase of 5−10% in the cell diameter when E_2 was 300 V/cm. The percentile increase in the cell diameter could go up to 48% when E_2 was 500 V/cm. The plateau in the 500 V/cm curve was mostly caused by the confinement of the channel walls. We often observed an abrupt increase in the cell diameter once the cells exit the narrow section when E_2 was 500 V/cm.

The cells typically went out of sight of the camera within 400 ms with E_2 at 500 V/cm. At this time scale, we did not observe complete disruption of the cell membrane (cell lysis). However, we were able to observe leaking of intracellular materials in some cases when the cells were loaded with fluorogenic calcein AM (data not shown).

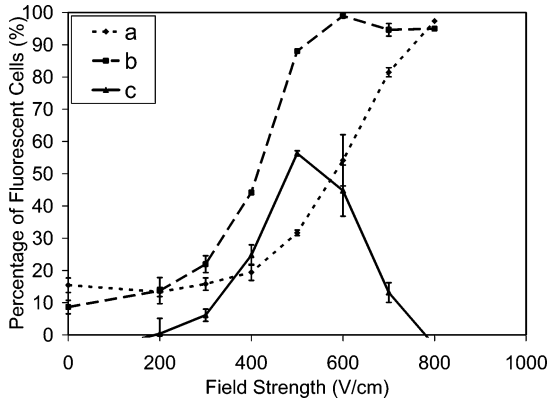

Figure 5. Electropermeabilization of cells to SYTOX green at varying E_2 and a fixed duration of exposure to E_2 at 40 ms. The two broken line curves show the percentage of fluorescent cells when SYTOX green was added before the electroporation (curve b) and 1 h after the electroporation (curve a). The solid line curve (curve c) is the difference between the other two curves and represents the percentage of cells that were electropermeabilized and remained viable.

Internalization of a Membrane-Impermeant Dye SYTOX Green. To further confirm that the electroporation occurred during the operation, we also demonstrated delivery of a membrane-impermeant dye SYTOX green into CHO cells using this device. SYTOX green is impermeant to live cells. It can enter compromised cell membrane, due to either cell death or electropermeabilization, then bind to nucleic acid, and become strongly fluorescent. In this experiment, we varied the field intensity E_2 in the narrow section and kept the duration of field exposure constant at 40 ms. We measured the percentage of fluorescent cells after the electroporation when the cells were first mixed with the dye and then flowed into the device for electroporation (Figure 5, curve b). The fluorescent labeled cells in this case included both dead cells and viable cells that were electropermeabilized. We then measured the percentage of fluorescent cells by adding the dye 1 h after the electroporation (Figure 5, curve a). In the second case, the fluorescent cells included only the dead cells since it is known that the internalization stops within several seconds after the field is removed.[42,43] Both the curves go up when the field intensity E_2 increases. Considering the standard deviation in the data points, there is no significant difference between curves a and b when E_2 is below 400 V/cm. The small percentage of stained cells (in both curves a and b) when E_2 is between 0 and 300 V/cm is mostly due to cell death, which may be partially related to the extended period (1.5 h) that the cells were placed in the electroporation buffer instead of a full medium at room temperature. Curve c indicates the difference between curves b and a, and it represents the percentage of the cells that was electropermeabilized during the process and remained viable after electroporation. Curve c increases first with the field intensity, peaks at 500 V/cm with ∼56% cells, which were electropermeabilized and viable, and then decreases. Eventually when E_2 was ∼800 V/cm, all the cells were dead after the electroporation.

(42) Rols, M.; Teissie, J. *Biophys. J.* **1990**, *58*, 1089−1098.
(43) Hibino, M.; Itoh, H.; Kinosita, K. *Biophys. J.* **1993**, *64*, 1789−1800.

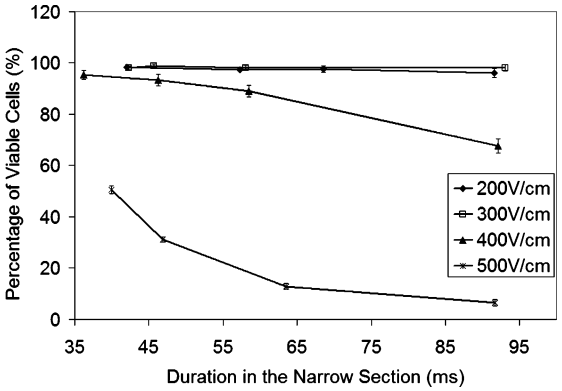

Figure 6. Effects of field strength and duration of E_2 (in the narrow section) on cell viability. Cell viability was determined by trypan blue exclusion 1 h after the electroporation.

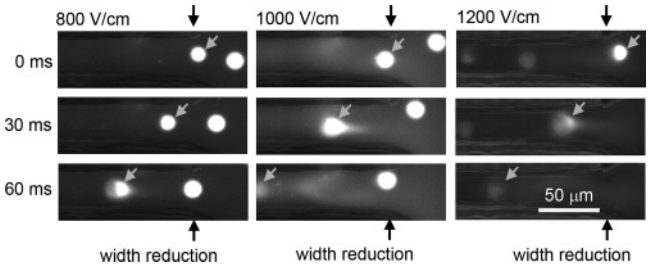

Figure 7. Image series showing the rapid release of intracellular materials when E_2 was between 800 and 1200 V/cm. The images were taken at a frame rate of 33 Hz. The arrows indicate where the width reduction occurs in the channel.

These results indicate that the internalization of exogenous molecules that were impermeant to the membrane did occur during the process. This suggests the potential of using our device for delivery of drugs and nucleic acids into cells while preserving cell viability. In principle, the duration of field exposure can be optimized to balance between the level of electropermeabilization and the preservation of cell viability.

Cell Viability after Electroporation. The duration for cells to be in the electroporation field E_2 could be adjusted by controlling the flow rate through the channel using a syringe pump. The velocity of cells in the narrow and wide sections of the device with different field strengths and infusion rates were determined based on time-resolved images of calcein AM-loaded cells (data not shown). We studied the effects of the field intensity and the duration in the field on cell viability. We did not observe serious adverse effects on cell viability even when cells experienced long durations (up to a couple of seconds) of the weak field E_1 in the wide sections ($E_1 = 1/6.5E_2$, less than 77 V/cm with E_2 at 500 V/cm or lower). Therefore, we believe that the magnitude and duration of E_2 were the most relevant parameters in the operation of the device. The duration for cells to be in the fields can be calculated based on the lengths of sections and the velocities of cells in them. We found that, when the duration in E_2 was less than 100 ms, the cells could have high survival rates with E_2 at 500 V/cm or lower. As shown in Figure 6, the cell viability was essentially unaffected when the field strength was lower than the threshold for electroporation (400 V/cm). The percentage of viable cells dropped from 95 to 68% when the duration in the field increased from 36 to 92 ms with E_2 at 400 V/cm. The percentage of survival was decreased further (from 51 to 7%) when E_2 became 500 V/cm. When E_2 was in the range of 200−300 V/cm, the viability was essentially 100%. There are discrepancies between the actual numbers in Figure 5 and Figure 6 when the operational conditions were the same, presumably due to the different working mechanisms of two dyes used (SYTOX green and trypan blue) when indicating cell viability.

It needs to be noted that the duration of field in this study was substantially longer than the typical pulse width used in electropulsation studies. Pulse widths of several microseconds to 20 ms have been normally used in electropulsation experiments when cell viability was desired. The velocity of cells in the electroporation field E_2 in our study was typically in the range of 2.0−5.0 cm/s. By decreasing the length of the narrow section, we will be able to reduce the duration of field to the level of several milliseconds easily. We expect that such practice will dramatically increase the cell survival rate. Our data suggest that our technique and device have the potential for applications related to delivery of drugs and genes during which cell viability needs to be preserved.

Rapid Cell Lysis in a High Field. We were able to observe cell lysis in real time when cells loaded with fluorogenic dye (calcein AM) entered the narrow section. As shown in Figure 7, such a process became more and more rapid when E_2 increased from 800 to 1200 V/cm. With E_2 at 1000 V/cm, most of intracellular contents were depleted at 60 ms after the cell entered the narrow section due to the disruption of the membrane. At 1200 V/cm, a similar process finished mostly within the first 30 ms. These results match the time scale for cell lysis reported in previous literature with similar field strength.[16] In Figure 7, the intracellular materials were eluted in the direction opposite of cell movement. Since the direction of cell movement was determined by the pressure-driven flow in our design, it would be trivial to reverse it to make the movement of cells and the elution of intracellular materials in the same direction. Such a configuration would be extremely convenient for single-cell analysis based on separation and detection methods such as electrophoresis coupled with laser-induced fluorescence.

When E_2 was 600 V/cm or higher, 100% of the cells were observed to be lysed within 150 ms after entering the narrow section. When E_2 was between 400 and 600 V/cm, cell lysis often did not happen or happened after a longer duration for a given cell. We enumerated the percentage of cells lysed within each elapsed frame (the interval between frames was 30 ms) at different E_2 (600, 800, 1000, and 1200 V/cm). In here we consider the onset of release of intracellular materials as the indication of cell lysis. Figure 8 shows that the average time for lysis to occur shifted to the shorter end when E_2 increased. More than 90% of the cells were lysed within 30 ms when E_2 was 1200 V/cm. In principle, our technique will allow easy integration with electrophoresis for carrying out chemical analysis of intracellular contents at the single-cell level, or "chemical cytometry".[19,29,44,45] Based on data from Figure 8, one will be able to design an appropriate length for the narrow section and optimize the velocity of cells to lyse all the cells by the time that they exit the device.

(44) Dovichi, N. J.; Hu, S. *Curr. Opin. Chem. Biol.* **2003**, *7*, 603−608.
(45) Wu, H. K.; Wheeler, A.; Zare, R. N. *Proc. Natl. Acad. Sci. U. S. A.* **2004**, *101*, 12809−12813.

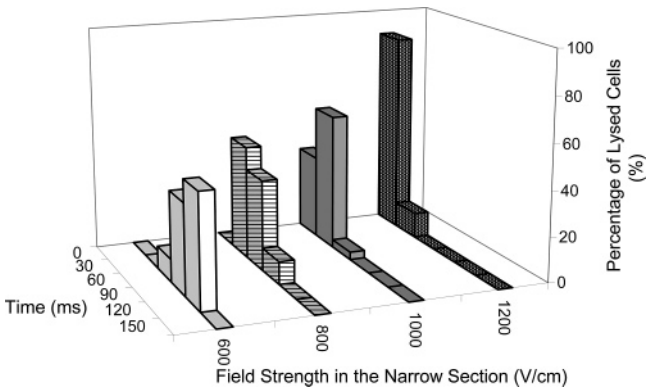

Figure 8. Percentage of cells lysed during the intervals between frames with different intensities for E_2. Each curve was obtained based on a sample size of at least 30 cells.

During electrical lysis of cells in the high field, special care needs to be taken to avoid excessive Joule heating, which may impair the biological activities of target biomolecules. With the isotonic buffer (10 mM phosphate and 250 mM sucrose) and the microfluidic channel used in this work, we had a current of 23 μA with E_2 at 600 V/cm and it increased to 51 μA with E_2 at 1200 V/cm. The current can be further suppressed by decreasing the concentration of the buffer, assuming that the biological properties of cells under study are not directly affected by the buffer concentration at the time scale needed for a rapid chemical cytometry analysis.

CONCLUSIONS

In this report, we demonstrated a simple microfluidic device for continuous-flow cell electroporation using a dc field. With geometric variation of a microfluidic channel, we were able to amplify the electrical field strength in a section of the channel and induce electroporation when cells flowed through the device. The expansion in the cell size during electroporation was observed in real time in the device. We also demonstrated the delivery of membrane-impermeant molecules into the cells during the electroporation. The duration for cells to experience the high field could be adjusted using pressure-driven flow. When the duration was in the range of 10−100 ms, a large portion of cells remained viable after electroporation. Rapid disruption of the membrane, or cell lysis, was observed when the electroporation field was 600 V/cm or higher. When the electroporation field was higher than 1000 V/cm, the majority of cells were lysed within 60 ms.

Our results indicated that an electrical field with intensity significantly lower than the electroporation threshold did not lead to severe cell death. The electroporation occurred only in a geometrically defined section of the device. Our technique provides a very simple solution to processing biological cells on a microfluidic platform. This method may find important applications in microfluidic delivery of drugs and genes and chemical cytometry analysis at the single-cell level.

ACKNOWLEDGMENT

We thank Dr. Ji-Xin Cheng for donating CHO-K1 cells. The research was supported by Bindley Bioscience Center at Purdue University and Purdue University.

Received for review April 18, 2006. Accepted April 21, 2006.

AC060733N